International Journal of Pharmaceutics 384 (2010) 148–153

Contents lists available at ScienceDirect

International Journal of Pharmaceutics

journal homepage: www.elsevier.com/locate/ijpharm

Pharmaceutical Nanotechnology

Preparation of nanobubbles for ultrasound imaging and intracelluar drug delivery

Ye Wang[a,*], Xiang Li[a], Yan Zhou[c], Pengyu Huang[a], Yuhong Xu[a,b]

[a] Zhejiang-California International Nanosystems Institute Molecular Imaging Platform, Zhejiang University, 268 Kaixuan Road, Hangzhou 310029, PR China
[b] School of Pharmacy, Shanghai Jiao Tong University, 800 Dongchuan Road, Shanghai 200240, PR China
[c] Shandong Provincial Research Center for Bioinformatic Engineering and Technique, 12 Zhangzhou Road, Zibo 255049, PR China

ARTICLE INFO

Article history:
Received 26 May 2009
Received in revised form
13 September 2009
Accepted 15 September 2009
Available online 23 September 2009

Keywords:
Nanobubbles
Ultrasound imaging
Cellular uptake
Drug delivery

ABSTRACT

Echogenic bubble formulations have wide applications in both disease diagnosis and therapy. In the current study, nanobubbles were prepared and the contrast agent function was evaluated in order to study the nanosized bubble's property for ultrasonic imaging. Coumarin-6 as a model drug was loaded into nanobubbles to investigate the drug delivery potential to cells. The results showed that the nanobubbles composed of 1% of Tween 80, and 3 mg/ml of lipid worked well as an ultrasonic contrast agent by presenting a contrast effect in the liver region *in vivo*. The drug-loaded nanobubbles could enhance drug delivery to cells significantly, and the process was analyzed by sigmoidally fitting the pharmacokinetic curve. It can be concluded that the nanobubble formulation is a promising approach for both ultrasound imaging and drug delivery enhancing.

1. Introduction

The development of nanomedicine has emerged with the marriage of nanotechnology and medicine (Sanhai et al., 2008). Nanovectors show significant importance for healthcare in both diagnostic and therapeutic applications, due to the many special features in nanosized particles. In the human body, nanoparticles could accumulate in organs and tissues important for diagnosis or therapy, such as the liver, spleen, and tumor tissues. A large number of polymeric nanoparticles were applied in basic and clinical medical studies. Many of them improved the drugs' distribution profile, which usually influenced positively the drug delivery properties (Farokhzad and Langer, 2006). In the diagnostic field, nanotechnology has impacted nearly all aspects of the imaging methodology. Nanoagents were designed and used as probes for the early detection of malignant diseases. There have been many papers published that demonstrated their applications in magnetic resonance (MR) (Sun et al., 2008), positron emission tomography (PET) (Lee et al., 2008), ultrasound (US) (Rapoport et al., 2007) imaging and others. It is believed that nanotechnology has led the diagnostic and therapeutic work into the molecular level.

Among the many novel nano-carriers being developed, echogenic bubble formulations have been gaining lots of attention in recent decades (Saad et al., 2008). Bubbles are filled with gas, spherically shaped and stable in aqueous (Ferrara et al., 2007). Compared to other particles, bubbles have the special properties of being "explosive" under ultrasound-energy illumination, prompting the destruction of bubbles and cellular membrane permeability changes. Various bubble formulations were used for local drug delivery (Bull, 2007), for gene delivery (Chen et al., 2003) and targeting drug delivery (Lum et al., 2006). They were developed based on micron-scale (μm) bubbles commercially available as ultrasound contrast agent for imaging diagnosis.

Besides drug delivery, bubbles have also attracted investigators on ultrasonic imaging work. Ultrasonic imaging is one of the most important technologies in medical diagnosis. It presents such advantages as freely utilizing, dynamic observing, real-time detecting, and the high priority of biological safety without radiocontamination.

Ultrasonic imaging has been demonstrated as a promising tool for diagnosis of many diseases, gas filled bubbles were always taken as ultrasonic contrast agents. In recent decade, nanobubbles were developed as the contrast agent or drug vector mainly for tumor-related molecular imaging by the size effect (Pitt et al., 2004; Liu et al., 2006). For example, octafluoropropane filled nanobubbles were generated by Span 60 and Tween 80, the bubble size ranged from 450 nm to 700 nm, this kind of nanobubbles displayed dose-response echo enhancement both *in vitro* (Oeffinger and Wheatley,

Abbreviations: SF_6, sulphur hexafluoride; UBM, ultrasonic biological microscopy; SPC, soybean lipid; CHO, cholesterol; DPPG, dipalmitoyl phosphatidylglycerol; MPP, sodium poly phosphate; CNP, chitosan nanoparticle; ROI, region of interest; TOI, time of interest; NBS, number of bright spots; MNTI, mean NBS of TOI; LiposomeA, the liposomes without Tween 80 modification.

* Corresponding author. Tel.: +86 571 86971897; fax: +86 571 86971897.
E-mail addresses: wangyeph@hotmail.com, wangyeph@yahoo.com.cn (Y. Wang).

0378-5173/$ – see front matter © 2009 Elsevier B.V. All rights reserved.
doi:10.1016/j.ijpharm.2009.09.027

2004) and *in vivo* (Wheatley et al., 2006). Nanobubbles contained perfluoropentane were confirmed to be stabilized by copolymer, it played as both drug delivery enhancers and ultrasonic contrast agents (Rapoport et al., 2007).

The bubbles were mainly used for blood pool imaging, and in certain applications, for imaging thrombus (Alonso et al., 2007), tumor (Mitterberger et al., 2007), inflammation (Lindner et al., 2000), etc. They were also modified to carry genes and peptides for delivery by ultrasound induced cavitation. However, the fact that micro-sized particles could only stay in blood pools and penetrate poorly in tumor tissues has restricted their applications for *in vivo* tumor therapy. In order to improve the contrast agents' biological function by nanotechnology, in this study, nanosized functional bubbles were designed and prepared, and the ultrasound imaging function and cellular delivery property of nanobubbles were investigated.

2. Materials and methods

2.1. Materials

SF_6 (sulphur hexafluoride) gas was purchased from Tomoe gases company (Shanghai, CHN), soybean lipid (SPC) was purchased from Lipoid (Toshisun Company, Shanghai, CHN), Tween 80 and cholesterol (CHO) were supplied by China National Medicine Cooperation Ltd. (Shanghai, CHN), coumarin-6 was purchased from Sigma (Sigma–Aldrich, USA). Other reagents were all analytical purified.

2.2. Apparatus

Ultrasonic emission instrument (40 kHz, 250 W, Fuyida, Kunshan, CHN), B-mode ultrasonic biological microscope (UBM, SUOER, Tianjin, CHN, Center frequency of transducer: 50 MHz), Nano-S90 Zetasizer (Malvern, Worcestershire, UK), Infinite M200 multifunctional plate reader (Tecan, Männedorf, Switzerland), MATLAB software (The MathWorks, Natick, MA, US), Origin software (OriginLab, Northampton, MA, USA).

2.3. Preparation of nanobubbles for contrast agent

The bubbles were prepared as following: a certain quantity of lipid and specified additives were mixed and dissolved in chloroform in a flask, the solvent was removed by reduced pressure vaporization. Residual lipid was then resuspended in saline until it turned homogeneous. Mixture loaded in the flask was then placed in the ultrasonic emission instrument for 5 min sonication. During this process, approximately 5 ml of SF_6 was introduced into the liquid mixture through a syringe. After sonication, the upper visible foam was quickly removed and the bubble suspension for ultrasound observation was acquired.

2.4. Formula influence of the nanobubbles

An investigation of three important components was carried out to set up the optimal formulation of the nanobubbles. Generally, soybean lipid (SPC) was chosen as the bubble film. Tween-80 and cholesterol (CHO) were added as the additives. Series of experiments were designed by changing one of the agents while the other two unvaried: (a) Tween 80 concentration was varied from 0% to 3%, meanwhile the lipid concentration was 5 mg/ml, and SPC: CHO was 8:1 (molar ratio). (b) Lipid concentration was varied from 1 mg/ml to 8 mg/ml, meanwhile Tween 80 concentration was 1%, and SPC: CHO is 8:1. (c) SPC: CHO was varied from 8:0 to 8:8, meanwhile Tween 80 concentration was 1%, and lipid concentration was 5 mg/ml.

2.5. In vitro ultrasonic imaging of bubbles and acoustic quality evaluation

The ultrasound contrast results were observed by a B-mode ultrasonic biological microscopy (UBM). This instrument could obtain the real-time ultrasonic signal and photos. A certain quantity of freshly prepared bubble formulation was transferred into a glass beaker, which was pre-covered with a layer of solid agarose to avoid the acoustic reflection of glass. The probe of the UBM was immersed into the liquid to get the ultrasonic image, the image photos were taken for 10 s to get 100 photos, with sampling interval of 0.1 s. For testing the *in vitro* ultrasonic effect, the quantity of bubbles in the view was taken as the evaluation standard of the contrast agent.

Matlab software was utilized for counting the bubbles of the UBM. In brief, the monochrome images in BMP format of bubbles were read-in through the Matlab workspace, and Simulink module of Matlab was edited to count the bubbles. The quantities were finally feedback to the workspace. 100 photos were counted for one sample to minimize the variation.

2.6. In vivo ultrasonic imaging

All the animal experiments in this work were carried out under the approval of Animal Care and Use Committee of Zhejiang University. In this part, a mouse was chosen to test the ultrasonic contrast effect of the bubbles *in vivo*. A female nude mouse was obtained from Slaccas (Shanghai, CHN) and used at 6 weeks. After *in vitro* formula screening of the above section, the optimized formulation was chosen for *in vivo* testing. 30 mg of SPC, CHO and DPPG were mixed and suspended in 10 ml of saline (1% Tween 80 contained) with the molar ratio of 8:1:1, sonicated by probe sonication. The final lipid concentration was 3 mg/ml. The prepared bubble formulations were injected into the nude mouse through the tail vein, the UBM probe was simultaneously placed at the liver region to investigate the contrast enhancement.

2.7. Drug load nanobubbles preparation

Coumarin-6 was chosen to be a model drug for cell testing. Drug-loaded nanobubbles were prepared similar to the above application, and analogous to Ferrara 's work (Tartis et al., 2006) by introducing oil phase to the preparing process. That is coumarin-6 dissolved in soybean oil, and the oil phase was then mixed with lipid solution (1:40, O/W, v/v). The other operations were the same as the prior preparing process. Final lipid concentration was 3 mg/ml.

Emulsion, liposome and chitosan nanoparticle (CNP) were also prepared for the cell test, they were taken as control agents for nanobubbles. Emulsion was prepared using the method of bubbles preparation without loading gas. Liposome was prepared through a widely used "film" method (Sezer et al., 2004). Briefly, 30 mg of SPC was dissolved in chloroform together with the drug, after that, the organic solvent was evaporated by a reduced pressure evaporator, then the residual film was washed by 10 ml of saline (contained 0.1% of Tween 80) to form the liposome. CNP was prepared through a crosslinking way. In brief, a certain quantity of drugs were dissolved in 1.5 ml of 0.1% sodium poly phosphate (MPP), and then the mixture was added into 8.5 ml of 0.5% chitosan acid solution dropwise until the opalescence emerged.

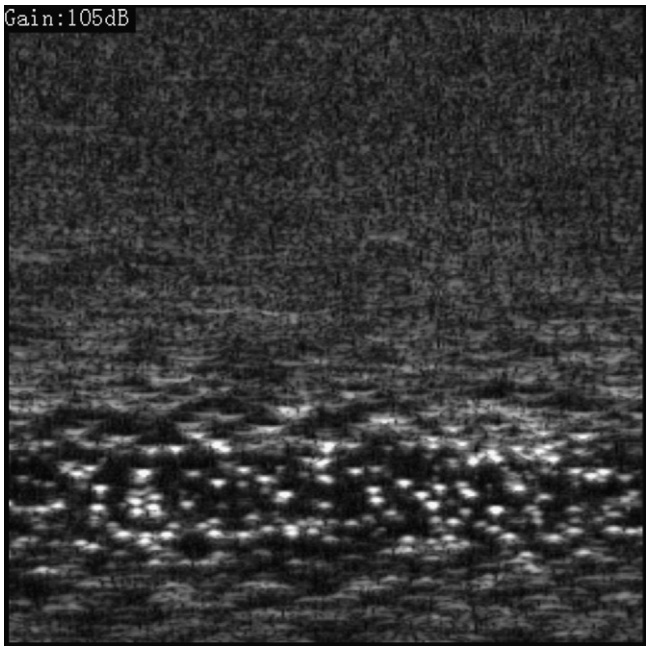

Fig. 1. The prepared nanobubbles presents as bright spots viewed by the UBM.

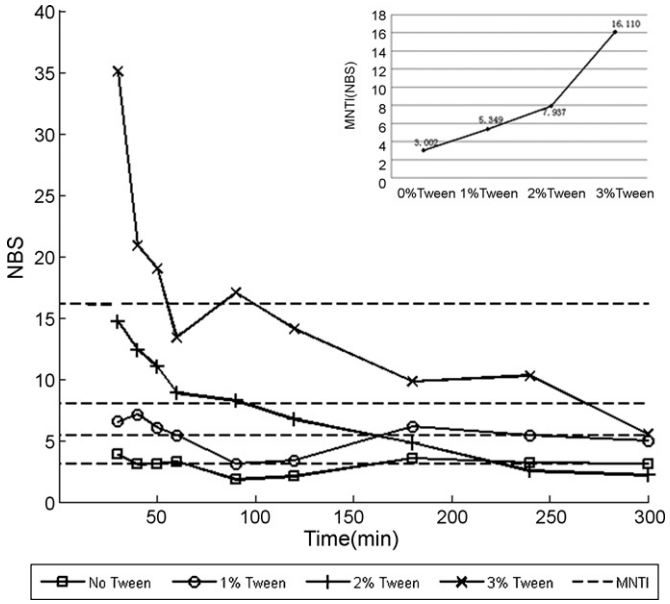

Fig. 2. Influence of Tween 80 on the acoustic property of nanobubbles. The solid line is the NBS actually counted, the dashed line is MNTI calculated based on NBS. MNTI is displayed in the corner figure.

In all of the preparations, the final concentration of coumarin-6 and lipid were 20 μg/ml and 3 mg/ml, respectively.

The particles sizes were analyzed by a Nano-S90 Zetasizer.

2.8. MCF-7 cell culture and vector mediated drug uptake

Coumarin-6 uptaken by tumor cells was estimated by quantifying the fluorescent drug concentration in the cells. Human breast carcinoma cells (MCF-7) were maintained in RPMI 1640 medium which contained 10% of fetal bovine serum, 1% of penicillin/streptomycin solution (10,000 IU/ml). Cells were cultured in a 96-well Costar plate at a density of 1×10^5 cells per well and placed in an incubator with 5% of CO_2. After 12 h of incubation, the cell plate was taken out of the incubator and 2 μl of formulation was added in each well. At predetermined intervals, the medium were fully withdrawn and discarded. The wells were then washed by PBS (pH 7.4) twice. Subsequently, 100 μl of cell lysis buffer was precisely added into the wells to lyse the cells. The lysate was then centrifugated (10,000 rpm, 5 min), 50 μl of supernatant was then added into a black opaque Costar assay plate to detect the concentration of coumarin-6 in an infinite M200 multifunctional plate reader. The excitation and emission wavelength were 456 nm and 504 nm, respectively.

Data analysis was performed by Origin software. A drug uptake curve was fitted by sigmoidal way, and correlated pharmacokinetic data were acquired from the equation of the sigmoidal curve.

3. Results

3.1. In vitro ultrasonic contrast observation of nanobubbles

Nanobubbles were detected by the UBM. Bubbles presented as bright spots in the focus region of the image (Fig. 1).

3.2. Nanobubbles acoustic quality evaluation

To quantify and investigate the influence factors precisely, four parameters were defined; (1) ROI (region of interest), this means the part of the focus region where is the brightest and clearest in the ultrasonic image. Equal area of ROI was chosen in every photo for calculating bubbles. (2) TOI (time of interest), this means the time interval actually cared during the investigation. In this experiment, TOI was 30–300 min. (3) NBS (number of bright spots), it is the number of bright spots in ROI calculated by Matlab. The bubbles' quantity was acquired by counting the NBS. The parameter reflects the gas content, the higher the NBS, the more bubbles in the formulation; (4) MNTI (mean NBS of TOI), this is the mean number of bright spots in TOI, which is also calculated by Matlab. The parameter reflects the mean gas content in the bubble formulation during a time interval, the higher the MNTI, the more stable of the bubbles.

High ratio of Tween 80 enhanced the acoustic backscatter property of bubbles. NBS increased from 3.002 to 16.110 as Tween 80 changed from 0% to 3% (Fig. 2).

Fig. 3 demonstrates the influence of cholesterol. The results showed high quantity of cholesterol gave negative contribution to

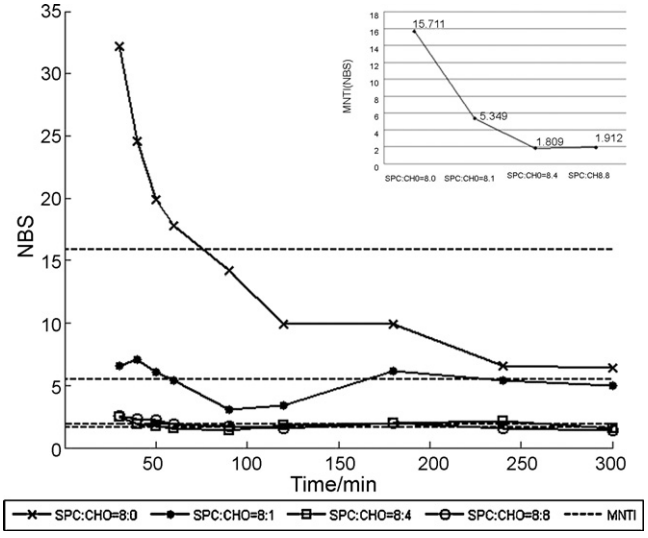

Fig. 3. Influence of cholesterol on the acoustic property of nanobubbles. The solid line is the NBS actually counted, the dashed line is MNTI calculated based on NBS. MNTI is displayed in the corner figure.

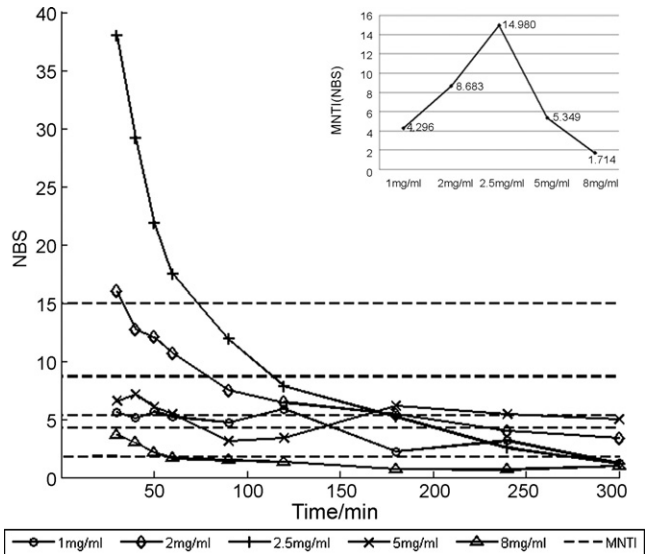

Fig. 4. Influence of lipid concentration on the acoustic property of nanobubbles. The solid line is the NBS actually counted, the dashed line is MNTI calculated based on NBS. MNTI is displayed in the corner figure.

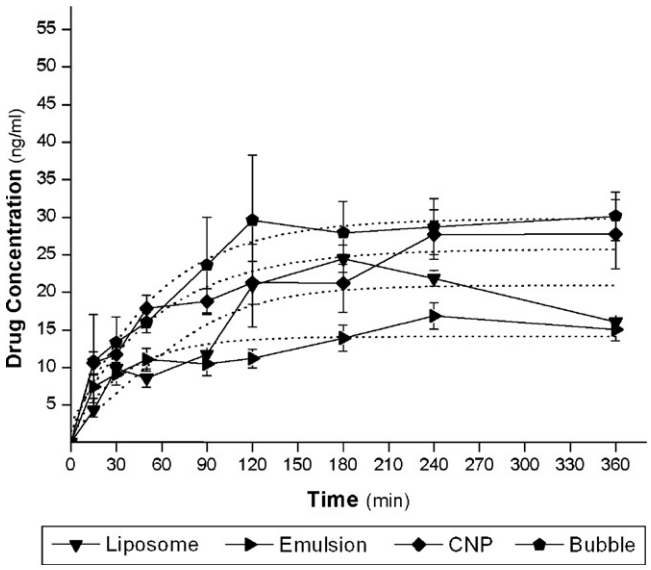

Fig. 6. Treated by different preparations, the coumarin-6 cell uptaken in MCF-7 cells. Solid line is the real-time depended drug concentration. The dash line is the fitted curve (mean ± SD, $n = 3$) (CNP represents chitosan nanoparticle).

the bubbles' acoustic property, and bubbles showed highest echo without cholesterol participated, which presented MNTI as 15.711.

When lipid was 2.5 mg/ml around, bubbles presented the best acoustic backscatter profile among the formulations tested. MNTI was 14.980 at lipid concentration of 2.5 mg/ml, while this parameter value decreased when the concentrations changed up or down (Fig. 4).

3.3. In vivo ultrasonic imaging

After injection, an area of echogenicity was seen in the liver region in the nude mouse tested, as shown in Fig. 5.

3.4. Tumor cell uptake of coumarin-6 loaded bubbles

For the pharmacokinetic process, only the absorption phase was examined. The drug absorption feature was analogized as pharmacokinetic data. The pharmacokinetic parameters were acquired by fitting the concentration variation into "S" curves, C_∞ and $t_{1/2}$ was calculated from the curve equation, k was defined as the reciprocal of $t_{1/2}$. Similar to other pharmacokinetic parameters, C_∞ indicates the final concentration (plateau concentration) of drugs and $t_{1/2}$ and k reflects the drug absorption rate. In the tested vector groups, nanobubbles showed preferable profile for intracellular drug uptaken (Fig. 6). Compared to chitosan nanoparticles, liposome and emulsion, the nanobubbles got the highest C_∞ (29.780 ng/ml), and the largest value of $t_{1/2}$ (35.4 min). Fig. 7 demonstrates the comparison of nanobubbles and liposomes. Liposome A represented the liposomes without modification of Tween 80. The result demonstrated that liposomes modified with 0.1% Tween 80 got higher C_∞ than general liposomes (liposome A).

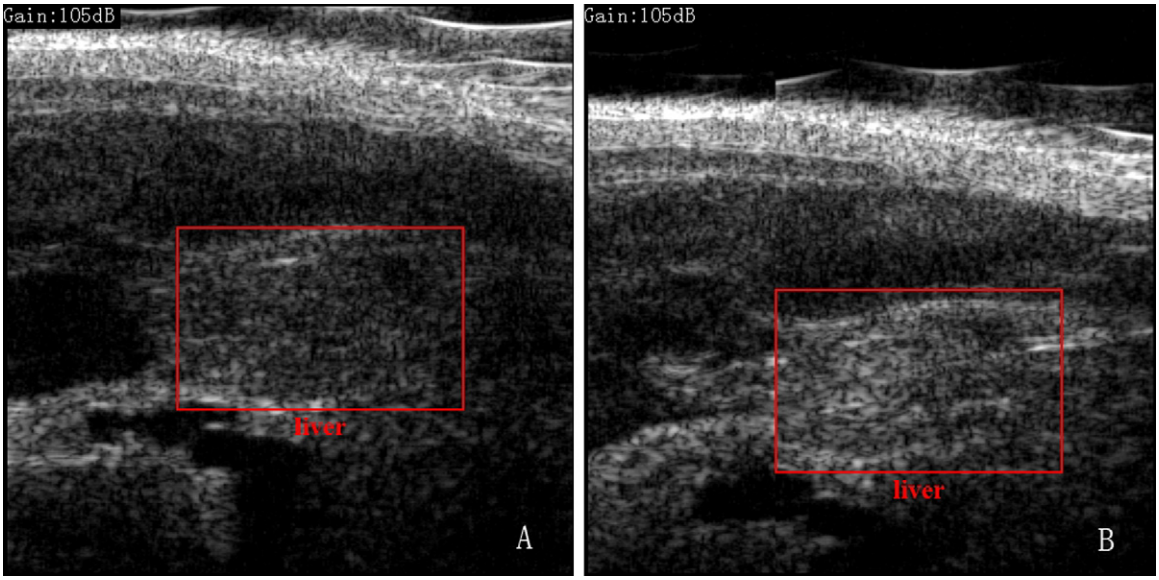

Fig. 5. B-mode ultrasound image of nanobubbles in a nude mouse after intravenous injection of bubble preparation, the red frame demonstrates the echo enhancement in the liver region. (A) Pre-injection; (B) post-injection. (For interpretation of the references to color in this figure legend, the reader is referred to the web version of the article.)

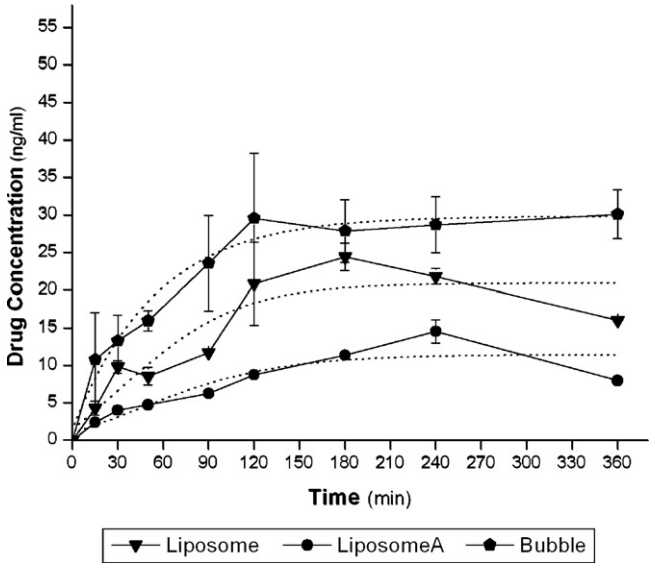

Fig. 7. Treated by Tween modified or no Tween added preparations, the coumarin-6 uptaken of in MCF-7 cells. The solid line is the real-time depended drug concentration. The dash line is the fitted curve (mean ± SD, $n = 3$) (liposome A represents the liposome without modification of Tween 80).

The detailed parameters were displayed in Table 1, the formulation particle size was also signed.

4. Discussion

Gas filled bubbles are commonly used as echo-enhancers in ultrasonic diagnosis (Calliada et al., 1998). Previously, contrast used bubbles were always prepared in micrometer size (Rychak et al., 2007; Willmann et al., 2008), because the echo signals are proportional to the bubbles' size (Phillips et al., 1998). Smaller dimensions always resulted lower resonance, and the bubble size and acoustic backscatter intensity is negatively correlated (Miller, 1981). So smaller particles in nanometer sized were thought not visible in ultrasonic imagers. In our study, we used an ultrasound microscope device with higher ultrasound frequency in order to characterize and optimize the nanobubbles echo intensities. In the *in vivo* ultrasonic imaging study, significant echo enhancement was seen in the liver region using this US imager. We believe it is because a large number of nanosized bubbles were phagocytized by abundant hepatic macrophages and the accumulation of nanobubbles resulted in significant acoustic backscatter.

For a stable nanobubble formation with significant echo intensity, we screened several formulations. Our experimental results indicated that the addition of Tween 80 could increase bubbles echo enhancement. It was speculated that the additives might have changed the bubble surface structure and improved the flexibility of the bubble shells. The high flexibility of nanobubbles might lead to the higher resonance frequency of bubbles approaching to the UBM frequency and presented echo enhancement at particles of 300–400 nm diameter. We chose the 1% Tween 80 formulation in our study instead of the 3% Tween one, because it was observed that higher ratios of Tween could cause the precipitation of bubble formulation during the test. SPC was the major component of the bubble shell, and the inclusion of cholesterol seemed to decrease the stability of bubbles.

Table 1
Particle size and pharmacokinetic parameters of preparations.

Name	C_∞ (ng/ml)	$t_{1/2}$ (min)	k (1/min)	R^2	Particle size (nm)
Nanobubble	29.78	35.40	0.028	0.972	333.1
Emulsion	14.09	21.60	0.046	0.864	397.2
Liposome	20.89	52.20	0.019	0.855	78.8
Liposome A	11.37	63.20	0.016	0.836	158.1
CNP	25.74	34.90	0.029	0.925	246.2

C_∞: the final drug concentration (plateau concentration); $t_{1/2}$: half-life of uptake; k: absorption rate constant; R^2: regression coefficient of curve equation.

The nanobubbles echo intensity also related to the total lipid concentration, mainly because the SF_6 entrapment efficiency increased with the lipid concentration increasing. But at high lipid concentrations, the formulation became instable and the nanobubbles might be destroyed, the resonance was decreased.

In addition to the echo enhancement properties, the nanobubbles we prepared were also tested for drug delivery potentials. Both liposome and emulsion are widely used for cellular drug delivery. In comparison, our nanobubble formulation showed even higher delivery efficiency as reported in Fig. 6. The nanobubbles significantly promoted the drug entry to the cells, even without external ultrasound-energy application as suggested by other studies (Dijkink et al., 2008). The cell test result demonstrated that the nanobubble formulation is a kind of promising drug vector.

The presence of Tween 80 in the formulation had been suggested to lead to enhancement in drug uptake (Liu et al., 1996; Kim et al., 2001). Our data in Fig. 7 also support this notion. Since Tween was shown to be also beneficial in nanobubble for imaging contrast enhancement, we believe the addition of Tween is crucial in this kind of dual-functional nanobubbles.

In summary, the nanobubbles reported in this paper can work as an ultrasound contrast agent and a drug delivery vector. Nanotechnology will allow earlier diagnosis and therapy, the combination of ultrasound imaging and drug delivery could be highly beneficial and may be achievable with further development of nanobubble formulations.

Acknowledgement

This work got the financial support of China Postdoctoral Science Foundation (No. 20070411202) by Ministry of Education of P.R.C.

References

Alonso, A., Della, M.A., Stroick, M., Fatar, M., Griebe, M., Pochon, S., Schneider, M., Hennerici, M., Allemann, E., Meairs, S., 2007. Molecular imaging of human thrombus with novel abciximab immunobubbles and ultrasound. Stroke 38, 1508–1514.
Bull, J.L., 2007. The application of microbubbles for targeted drug delivery. Expert. Opin. Drug Deliv. 4, 475–493.
Calliada, F., Campani, R., Bottinelli, O., Bozzini, A., Sommaruga, M.G., 1998. Ultrasound contrast agents: basic principles. Eur. J. Radiol. 27 (2 Suppl.), S157–S160.
Chen, S., Shohet, R.V., Bekeredjian, R., Frenkel, P., Grayburn, P.A., 2003. Optimization of ultrasound parameters for cardiac gene delivery of adenoviral or plasmid deoxyribonucleic acid by ultrasound-targeted microbubble destruction. J. Am. Coll. Cardiol. 42, 301–308.
Dijkink, R., Le, G.S., Nijhuis, E., van den, B.A., Vermes, I., Poot, A., Ohl, C.D., 2008. Controlled cavitation-cell interaction: trans-membrane transport and viability studies. Phys. Med. Biol. 53, 375–390.
Farokhzad, O.C., Langer, R., 2006. Nanomedicine: developing smarter therapeutic and diagnostic modalities. Adv. Drug Deliv. Rev. 58, 1456–1459.
Ferrara, K., Pollard, R., Borden, M., 2007. Ultrasound microbubble contrast agents: fundamentals and application to gene and drug delivery. Annu. Rev. Biomed. Eng. 9, 415–447.
Kim, T.W., Chung, H., Kwon, I.C., Sung, H.C., Jeong, S.Y., 2001. Optimization of lipid composition in cationic emulsion as in vitro and in vivo transfection agents. Pharm. Res. 18, 54–60.
Lee, H.Y., Li, Z., Chen, K., Hsu, A.R., Xu, C., Xie, J., Sun, S., Chen, X., 2008. PET/MRI dual-modality tumor imaging using arginine-glycine-aspartic (RGD)-conjugated radiolabeled iron oxide nanoparticles. J. Nucl. Med. 49, 1371–1379.
Lindner, J.R., Dayton, P.A., Coggins, M.P., Ley, K., Song, J., Ferrara, K., Kaul, S., 2000. Noninvasive imaging of inflammation by ultrasound detection of phagocytosed microbubbles. Circulation 102, 531–538.
Liu, F., Yang, J., Huang, L., Liu, D., 1996. Effect of non-ionic surfactants on the formation of DNA/emulsion complexes and emulsion-mediated gene transfer. Pharm. Res. 13, 1642–1646.

Liu, J., Levine, A.L., Mattoon, J.S., Yamaguchi, M., Lee, R.J., Pan, X., Rosol, T.J., 2006. Nanoparticles as image enhancing agents for ultrasonography. Phys. Med. Biol. 51, 2179–2189.
Lum, A.F., Borden, M.A., Dayton, P.A., Kruse, D.E., Simon, S.I., Ferrara, K.W., 2006. Ultrasound radiation force enables targeted deposition of model drug carriers loaded on microbubbles. J. Control. Release 111, 128–134.
Miller, D.L., 1981. Ultrasonic detection of resonant cavitation bubbles in a flow tube by their second-harmonic emissions. Ultrasonics 19, 217–224.
Mitterberger, M., Pelzer, A., Colleselli, D., Bartsch, G., Strasser, H., Pallwein, L., Aigner, F., Gradl, J., Frauscher, F., 2007. Contrast-enhanced ultrasound for diagnosis of prostate cancer and kidney lesions. Eur. J. Radiol. 64, 231–238.
Oeffinger, B.E., Wheatley, M.A., 2004. Development and characterization of a nano-scale contrast agent. Ultrasonics 42, 343–347.
Phillips, D., Chen, X., Baggs, R., Rubens, D., Violante, M., Parker, K.J., 1998. Acoustic backscatter properties of the particle/bubble ultrasound contrast agent. Ultrasonics 36, 883–892.
Pitt, W.G., Husseini, G.A., Staples, B.J., 2004. Ultrasonic drug delivery—a general review. Expert. Opin. Drug Deliv. 1, 37–56.
Rapoport, N., Gao, Z., Kennedy, A., 2007. Multifunctional nanoparticles for combining ultrasonic tumor imaging and targeted chemotherapy. J. Natl. Cancer Inst. 99, 1095–1106.
Rychak, J.J., Graba, J., Cheung, A.M., Mystry, B.S., Lindner, J.R., Kerbel, R.S., Foster, F.S., 2007. Microultrasound molecular imaging of vascular endothelial growth factor receptor 2 in a mouse model of tumor angiogenesis. Mol. Imaging 6, 289–296.
Saad, M., Garbuzenko, O.B., Ber, E., Chandna, P., Khandare, J.J., Pozharov, V.P., Minko, T., 2008. Receptor targeted polymers, dendrimers, liposomes: which nanocarrier is the most efficient for tumor-specific treatment and imaging? J. Control. Release 130, 107–114.
Sanhai, W.R., Sakamoto, J.H., Canady, R., Ferrari, M., 2008. Seven challenges for nanomedicine. Nat. Nanotechnol. 3, 242–244.
Sezer, A.D., Bas, A.L., Akbuga, J., 2004. Encapsulation of enrofloxacin in liposomes I: preparation and in vitro characterization of LUV. J. Liposome Res. 14, 77–86.
Sun, C., Fang, C., Stephen, Z., Veiseh, O., Hansen, S., Lee, D., Ellenbogen, R.G., Olson, J., Zhang, M., 2008. Tumor-targeted drug delivery and MRI contrast enhancement by chlorotoxin-conjugated iron oxide nanoparticles. Nanomedicine 3, 495–505.
Tartis, M.S., McCallan, J., Lum, A.F., LaBell, R., Stieger, S.M., Matsunaga, T.O., Ferrara, K.W., 2006. Therapeutic effects of paclitaxel-containing ultrasound contrast agents. Ultrasound Med. Biol. 32, 1771–1780.
Wheatley, M.A., Forsberg, F., Dube, N., Patel, M., Oeffinger, B.E., 2006. Surfactant-stabilized contrast agent on the nanoscale for diagnostic ultrasound imaging. Ultrasound Med. Biol. 32, 83–93.
Willmann, J.K., Paulmurugan, R., Chen, K., Gheysens, O., Rodriguez-Porcel, M., Lutz, A.M., Chen, I.Y., Chen, X., Gambhir, S.S., 2008. US imaging of tumor angiogenesis with microbubbles targeted to vascular endothelial growth factor receptor type 2 in mice. Radiology 246, 508–518.